

Expression and Cellular Localization of a Modified Type 1 Ryanodine Receptor and L-Type Channel Proteins in Non-Muscle Cells

B.S. Lee¹, S. Sessanna, S.G. Laychock, R.P. Rubin

Department of Pharmacology & Toxicology, The State University of New York at Buffalo, School of Medicine & Biomedical Sciences, Buffalo, NY 14214, USA

Received: 11 March 2002/Revised: 17 June 2002

Abstract. Functional and molecular biological evidence exists for the expression of ryanodine receptors in non-muscle cells. In the present study, RT-PCR and 5'-rapid amplification of cDNA 5'-end (5'-RACE analysis) provided evidence for the presence of a type 1 ryanodine receptor/Ca²⁺ channel (RyR₁) in diverse cell types. In parotid gland-derived 3-9 (epithelial) cells, the 3'-end 1589 nucleotide sequence for a rat RyR shared 99% homology with rat brain RyR₁. Expression of this RyR mRNA sequence in exocrine acinar cells, endocrine cells, and liver in addition to skeletal muscle and cardiac muscle, suggests wide tissue distribution of the RyR₁. Positive identification of a 5'-end sequence was made for RyR₁ mRNA in rat skeletal muscle and brain, but not in parotid cells, pancreatic islets, insulinoma cells, or liver. These data suggest that a modified RyR₁ is present in exocrine and endocrine cells, and liver. Western blot analysis showed L-type Ca²⁺ channel-related proteins in parotid acinar cells, which were of comparable size to those identified in skeletal and cardiac muscle, and in brain. Immunocytochemistry carried out on intact parotid acini demonstrated that the dihydropyridine receptor was preferentially co-localized with the IP₃ receptor in the apical membranes. From these data we conclude that certain non-muscle cells express a modified RyR₁ and L-type Ca²⁺ channel proteins. These receptor/channels may play a role in Ca²⁺ signaling involving store-operated Ca²⁺ influx via receptor-mediated channels.

Key words: Ryanodine receptor — IP₃ receptors — L-type channels — Dihydropyridine receptors — Parotid cells — Immunofluorescence

Introduction

Ca²⁺ mobilization through receptor-integral Ca²⁺ channels such as the inositol 1,4,5-trisphosphate receptor (IP₃R) and ryanodine receptor (RyR) is important in regulating Ca²⁺ levels and cell activation in diverse cell types. The RyR/Ca²⁺ channel complex, a homotetramer with a molecular weight of approximately 560 kDa, was originally identified by binding to the plant alkaloid ryanodine. The RyRs have been divided into three subtypes. RyR₁ and RyR₂ are enriched in skeletal muscle and cardiac muscle, respectively, and are well-characterized in these tissues (Sutko & Airey, 1996). RyR₃ has been cloned and identified in such tissues as brain and smooth muscle (Giannini et al., 1992). The basic RyR subtypes have several common structural features including the large N-terminal domain comprising the foot region, and the transmembrane domain near the C-terminus that is presumed to form the cation channel. The modulatory region between the N-terminal and the transmembrane domain contains the binding domains of Ca²⁺, adenine nucleotides, and calmodulin (CaM), as well as phosphorylation sites that may modulate receptor function. The different RyR isoforms are products of distinct genes and share a significant degree (60–70%) of amino acid sequence identity, particularly in the carboxyl-terminal region (Takeshima, 1993; Sutko & Airey, 1996). Despite the fact that the carboxyl-terminal region (3'-end) represents only 20% of the full-length RyR₁, this domain can by itself operate as a functional Ca²⁺ release channel (Bhat et al., 1997a,b). These findings are compatible with the concept that the carboxyl-terminal end of the RyR constitutes the pore of the Ca²⁺ release channel.

Comprehension of RyR function depends on acknowledging that there are important differences in the way RyR channels are regulated. In cardiac muscle, surface membrane dihydropyridine-sensitive

Correspondence to: R.P. Rubin; email: rprubin@acsu.buffalo.edu

¹Present address: Mitokor, 11494 Sorrento Valley Road, San Diego, CA 92121

(L-type) channels (DHPR) mediate the influx of a small amount of Ca^{2+} during depolarization that activates RyR₂ to release additional Ca^{2+} (i.e., CICR) (Franzini-Armstrong & Protasi, 1997; Franzini-Armstrong, Protasi & Ramesh, 1999). Excitation-contraction coupling in mammalian skeletal muscle occurs by depolarization of the T-tubule membrane, which leads to Ca^{2+} release from the sarcoplasmic reticulum (Franzini-Armstrong & Protasi, 1997). In this process the DHPR in close association with the foot region of the RyR₁ functions as a voltage sensor, which in response to depolarization activates the RyR₁ by a mechanism that does not require Ca^{2+} influx but involves direct protein-protein interactions (Franzini-Armstrong et al., 1999).

During the last several years, the existence of RyRs in non-excitable mammalian cells, including lung, renal, and exocrine acinar cells, has been established (Giannini et al., 1995; Bennett et al., 1996; Tunwell & Lai, 1996; DiJulio et al., 1997; Leite et al., 1999; Zhang et al., 1997, 1999). While high expression of RyRs typically occurs in muscle cells (Shoshan-Barmatz & Ashley, 1998), the level of expression of RyR in most non-excitable cells is very low (Bennett et al., 1996), frequently making their detection difficult. In an earlier study, a RyR/channel with distinct properties was identified in rat parotid acinar cells (Zhang et al., 1997, 1999). The sequence of this RyR showed high sequence identity to ~ 240 nucleotides of the 3'-end of the RyR₁ gene previously identified in rabbit brain (Takeshima et al., 1993; Zhang et al., 1997).

In the present study, a transcript identified by RT-PCR in exocrine and endocrine cells, as well as liver, was found to contain elements homologous to the 3'-region of the RyR₁ gene (Takeshima et al., 1993). A determination of the RyR partial sequence in rat parotid cell cultures by RT-PCR and rapid amplification of cDNA 5'-end (5'-RACE analysis) confirmed the presence of a RyR similar to that in rat brain and extended the sequence to 1589 bases. However, preliminary evidence indicates that the nucleotide sequence of the RyR in parotid and certain other tissues is not identical to skeletal muscle RyR₁ at the 5'-end. We also report in this study that parotid cells possess at least two L-type Ca^{2+} channel-related cell proteins in common with muscle cells that appear to preferentially co-localize with inositol 1,4,5-trisphosphate (IP_3) receptors. The unique localization of the DHPR and the divergent properties of the RyR presages a novel mechanism involved in the physiological regulation of Ca^{2+} signaling.

Materials and Methods

RyR RT-PCR

Total RNA was isolated from various tissues and cells with TRIzol reagent according to the manufacturer's protocol (GIBCO-Life

Technologies, Grand Island, NY). The RNA was used for RT-PCR and 5'-RACE. For RT-PCR, total RNA was treated with DNase and reverse-transcribed by using a first strand cDNA synthesis kit according to the manufacturer's instructions (GIBCO). Rat RyR₁-specific primers were designed on the basis of comparative sequence of novel mouse brain RyR₁ and the partial sequence of rat skeletal muscle RyR₁ that was provided by Dr. Deborah Bennett (Cambridge University, UK) (Zhang et al., 1997). The sequences of the sense (+) and antisense (-) primer pairs used for specific amplification of rat type I, II, III ryanodine receptors were: RyR₁ carboxyl-terminal end (+) 5'-GGTGGCCTCAACCTCT TCC-3' and (-) 5'-ACTTGCTCTTGGTCTCG-3' (287 bp); RyR₁ amino-terminal end (+) 5'-TCTGATTGAGAGTCCTGA GGTG-3' and (-) 5'-CATCACCTCGAAGTACCACTG-3' (301 bp); RyR₂ (+) 5'-GAGAACTATCCTGTCTCAG-3' and 5'-CTTGCTCTTGGTCTCTG-3' (380 bp); RyR₃ (+) 5'-GTTG CAACCTGTGGAACTC-3' and 5'-CTACTGGGCTAAAGTCA AGG-3' (430 bp). Mouse primers for RyR₁ (+) 5'-GAGAGGA GAGATAGTGTGTG-3' and (-) 5'-ACTGTGGTGCCTGAG TCCTC-3'; RyR₂ (+) 5'-TCGTGAGGATGCTCAGCCTG-3', and (-) 5'-CCTCTTCGCCTCTGCTCC-3'; RyR₃ (+) 5'-GATGATGACGAGGAAGAACG-3', and (-) 5'-CCAGG-CAAGGTAGAGAAAGG-3'. Using these primers, RyR cDNAs were amplified by PCR with a thermocycler (Model 2400, Perkin Elmer or Hybaid PCR Sprint) for 35–45 cycles with 1 unit of Pfu, Taq or Platinum Pfx polymerase. Reactions were carried out as follows: denaturation for 1 min at 95°C, annealing for 2 min at 60°C, and extension for 2.5 min at 74°C. For RyR₁ the reactions consisted of a 2-min initial denaturation, then 30 sec at 94°C, 30 sec at 55°C, and 1 min at 72°C. An aliquot of each PCR reaction was subjected to electrophoresis through a 1.5% agarose gel, and DNA was visualized by ethidium bromide staining. The DNA products were purified and sequenced in both directions by the CAMBI Nucleic Acid Facility (DNA Sequencing Service, The University at Buffalo).

RAPID AMPLIFICATION OF 5'-cDNA ENDS (5'-RACE)

Total RNA (~ 2.5 μg) isolated from parotid 3-9 cells as described above was used as a template for the 5'-RACE procedure, which was carried out according to the manufacturer's instructions (GIBCO-Life Technologies). Gene-specific cDNAs were purified using spin columns, and then tailed with poly-C using terminal deoxynucleotidyl transferase. After first-strand DNA synthesis, sequences were amplified for 35 cycles using the RyR₁-specific antisense primer 5'-ACTTGCTCTTGGTCTCG-3', and the universal anchor primer supplied in the kit. Nested gene-specific antisense primer (5'-GACGACCCGGTACAGTTCAT-3') and nested anchor primer confirmed the sequence. The thermal cycling conditions for the RT-PCR procedure consisted of an initial denaturation step for 2 min at 94°C, followed by 30 sec at 94°C, annealing at 55°C for 30 sec, and extension at 72°C for 2 min. PCR products were analyzed on a 1% agarose gel using 100 bp DNA ladder molecule markers. DNA bands were excised from the gel and sequenced directly as described above. A control reaction was performed with parotid mRNA in the absence of reverse transcriptase to eliminate the possibility of amplification due to genomic DNA contamination.

WESTERN BLOTH ANALYSIS

An antibody previously shown to recognize the α_1 subunit of muscle and neuronal voltage-gated Ca^{2+} channels (Hell et al., 1993) was used to detect similar proteins in non-muscle cells. Parotid cells were prepared by sequential digestion with trypsin and collagenase of freshly isolated parotid glands from two rats as

described previously (Rubin & Adolf, 1994). A homogenate fraction from these cells was subjected to electrophoresis (5% gel) and subsequently electrophoretically transferred to a polyvinylidene difluoride (PVDF) membrane. After the membrane was blocked with phosphate-buffered saline (PBS) plus 8% non-fat dry milk and 0.2% Tween-20, it was incubated with Ca^{2+} channel antibody anti- α_{1C} (1:1000) (Alomone Labs, Jerusalem, Israel) in PBS plus 8% milk. The primary antibody reaction was carried out at room temperature overnight. After immunoreactivity was visualized using peroxidase-conjugated secondary antibody, the blot was processed for enhanced chemiluminescence (ECL) (Pierce, Rockford IL, USA) and exposed to X-ray film.

IMMUNOFLUORESCENCE ANALYSIS OF DHPR

Initially 5–10 μm thick frozen sections of rat parotid gland were fixed for 10 min with 2% paraformaldehyde in PBS (pH 7.4), followed by 10 min of permeabilization with 0.1% Triton X-100. After being treated for 30 min with PBS and washed three times with PBS, the sections were blocked for 1 hr with 5% BSA in PBS. For immunofluorescence localization of DHPR, the primary antibody reaction was performed using Ca^{2+} channel antibody α_{1C} (1:200 or 1:2000) in PBS containing 5% BSA plus 0.1% Triton X-100 and incubated for 3 hr at 37°C. The sections were then washed 3 times with PBS containing 0.1% Triton X-100, and reacted in total darkness with secondary antibody (anti-rabbit 1:100) conjugated to fluorescein. After the sections were washed three times with PBS containing 0.1% Triton X-100 and covered with Prolong Antifade Reagent (Bio-Rad), they were initially viewed using epifluorescence optics of a Nikon upright Optiphot microscope. Confocal imaging was then performed with a laser scanning microscopy system (Model MRC-1024; Bio-Rad) configured with a Nikon microscope and a krypton-argon laser (488 nm). A 60 \times oil immersion objective was first employed to provide an overall view, and then zoom 2.64 \times optics yielded a high-magnification view. The system was operated by a Compaq pentium 100 computer and photographs were processed using a disublimation printer. Specificity of immunofluorescence was determined by incubating secondary antibody alone before microscopic analysis or by mixing antibody with its corresponding peptide prior to incubation. Immunofluorescence analysis of IP_3R was also carried out by confocal microscopy as previously described using a 1:20 dilution of affinity-purified IP_3R subtype II rabbit polyclonal antisera (Zhang et al., 1999).

Results

CHARACTERIZATION OF RyR mRNA IN VARIOUS CELL TYPES

In a previous study (Zhang et al., 1997), an RT-PCR product amplified in the 3'-end region of RyR₁ mRNA of rat parotid cells was sequenced and demonstrated by multiple sequence alignment to be similar to the RyR₁ sequence in rabbit, human, and mouse mRNAs. In the present study, RT-PCR analysis provided evidence that rat brain-type RyR₁ mRNA is also expressed in several tissues and cell types. In addition to parotid acinar cells, an RT-PCR product of expected size (287 bp) for the carboxyl-terminal 3'-end of RyR₁ was identified in rat skeletal muscle, cardiac muscle, brain, anterior pituitary (GH₃) cells, islets of Langerhans, RINm5F and

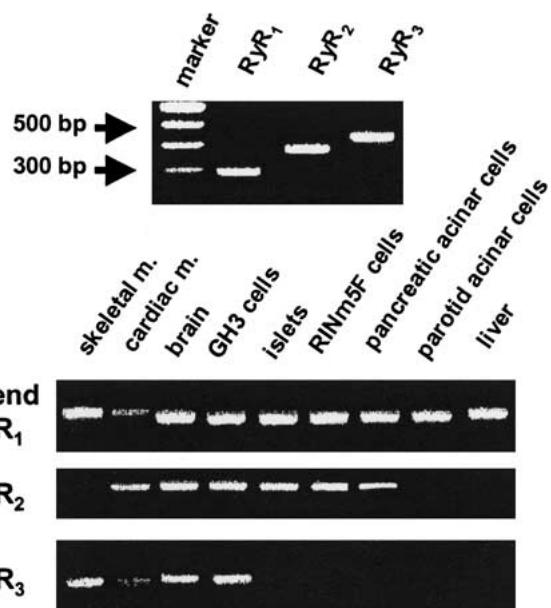


Fig. 1. Expression of RyR mRNAs in various tissue and cell types. Primers to the 3'-end of RyR₁, RyR₂ and RyR₃ were amplified by RT-PCR using RNA isolated from skeletal muscle (*m.*), cardiac muscle, brain, and other tissues or cells as indicated. The relative sizes of the RyR amplified products are shown in the top panel, where the first lane shows nucleotide size markers (*marker*). The results shown are representative of 3 separate experiments.

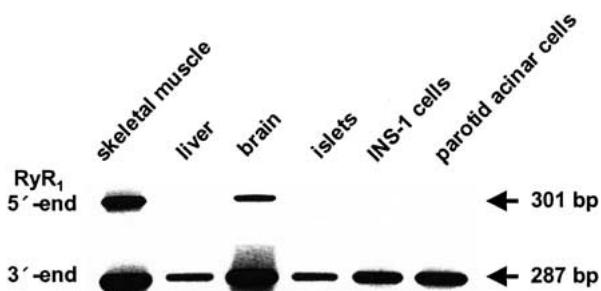


Fig. 2. Unique expression of 3'- and 5'-end RyR₁ mRNA in various cell types. RT-PCR amplification of mRNA was carried out for mRNA extracted from several rat tissues and cells as indicated, including islets of Langerhans (islets), insulinoma (INS-1) cells, and parotid acinar 3-9 cells. PCR primers targeted either the carboxyl-terminal (3'-end) or amino-terminal (5'-end) of rat RyR₁. PCR product was not detected in samples to which no reverse transcriptase was added (*not shown*). The size of the amplified products is indicated at the right hand margin. Similar results were obtained in two to four experiments.

INS-1 insulinoma cells, pancreatic acinar cells, and liver (Figs. 1, 2). In contrast, amplification of a rat skeletal muscle RyR₁ gene sequence located near the amino-terminal 5'-end identified a PCR product of 301 bp in cDNA from rat skeletal muscle and brain. However, the RyR₁ 5'-end primers failed to amplify cDNA from parotid acinar 3-9 cells, islets of Langerhans, INS-1 insulinoma cells, and liver (Fig. 2).

rRyR 1	gggtgaactgaaagtacagagagtgaattcttgaactacttgcaggaaacttctacac	60
mRyR 11	gggtgaactgaaagtacagagagtgaattcttgaactacttgcaggaaacttctacac	70
rRyR 61	gctgcgatccctggcccttcttcgttgcatttgcataactttatcttattgtttataa	120
mRyR 71	actgcgttccctggcccttcttcgttgcatttgcataactttatcttattgtttataa	130
rRyR 121	ggtttcagactctccgcacggggaggatgacatagaagggtccggagctggggacatgtc	180
mRyR 131	ggtctcagactctccaccacggggaggatgacatagaagggtccgggtctggggacatgtc	190
rRyR 181	agggcaagggtctggatggctctggctggggctccagagccagcgaggagtagagg	240
mRyR 191	agggca-gggtctggatggctctggctggggctccagggccggcaggagtagagg	249
rRyR 241	gtgatgaaatgagaacatgggtacttcttgcggagagcacccggctacatggaa	300
mRyR 250	gcgtatgaaatgagaacatgggtacttcttgcggagagcacccgg-ctacatggag	308
rRyR 301	cctgccttgagggtcttgcgcctgtgcatacoctggcccttctgcatttgcatttgc	360
mRyR 309	cctgccttgagggtcttgcgcctgtgcatacgcgtggcccttctgcatttgcatttgc	368
rRyR 361	tacaactgtctcaagggtccccctgtatcttaaggagagaaggagctggccggaaag	420
mRyR 369	tacaactgtctcaagggtccccctgtatcttaaggagagaaggagctggccggaaag	428
rRyR 421	ctggagggttcgttgcatttacattacagagccagggatgtatgtgaaaggagacag	480
mRyR 429	ctggagggttcgttgcatttacattacagagccagggatgtatgtgaaaggagacag	488
rRyR 481	tgggatcgctgtgtcaacacacccgtttcccccagcaactactggacaagttgtc	540
mRyR 489	tgggacccgttgcgtcaacacacccgtttcccccagcaactactggacaagttgtc	548
rRyR 541	aaggcaagggttctggacaaacacggggacatcttgcggggagcggattgcagagctg	600
mRyR 549	aaggcaagggttctggacaaacacggggacatcttgcggggagcggattgcagagctg	608
rRyR 601	ctgggcatggatctggcttotctggagatcacggccacaatgagcgcacccgttgcaccc	660
mRyR 609	ctaaatataatcttacccatcttacacacqccccaatgaccqccaaacctqaccct	668

The failure to identify a homologous region of the amino-terminal end of the RyR₁ gene in the latter tissues and cells suggests that the 5'-end of a skeletal muscle-type RyR₁ sequence is not common to all tissues, and points to a unique sequence or structure in the amino-terminal region of RyR₁ in some tissues.

Analysis of RyR₂ and RyR₃ mRNA expression was also carried out to determine tissue specificity among these receptor subtypes. RyR₂ mRNA was identified in pancreatic acinar cells and islets and RINm5F cells (Fig. 1), confirming the presence of authentic RyR₂ in these tissues as previously reported (Holz et al., 1999; Leite et al., 1999). RyR₂ mRNA was also identified in GH₃ cells, brain and cardiac muscle (Fig. 1). In contrast, RyR₂ mRNA was not identified in parotid acinar cells, skeletal muscle or liver (Fig. 1). RyR₃ mRNA was identified in GH₃ cells (Fig. 1), which coincided with evidence for RyR₃ in rat anterior pituitary glands (Sundaresan et al., 1997). RyR₃ mRNA was also identified in skeletal muscle, cardiac muscle, and brain, but not in parotid acinar cells, pancreatic acinar cells, pancreatic islets, RINm5F cells, or liver (Fig. 1).

Mouse tissues reflected the observed RyR mRNA expression in rat tissues. As expected, mouse

brain expressed skeletal muscle type RyR₁, RyR₂, and RyR₃ mRNAs (*data not shown*). Similar to rat islets and RINm5F cells, murine βHc9 insulinoma cells also expressed the 3'-end of RyR₁ and RyR₂ (*data not shown*).

5'-RACE AND SEQUENCE ANALYSIS USING PAROTID ACINAR CELLS

The previously published partial sequence of the 3'-end of rat RyR₁ extended only to 293 bp (Zhang et al., 1997). To further determine the sequence of the ubiquitously distributed RyR₁ isoform, 5'-RACE, i.e., rapid amplification of the cDNA 5'-end, was utilized for sequence analysis of cultured parotid (3-9) cells. The continuous epithelial cell line generated by stable transfection of freshly prepared rat parotid acinar cells developed in our laboratory retains the basic structural and functional properties of primary culture epithelial cells after treatment with rat serum (Zhu et al., 1998). Primers were designed to amplify discrete domains of the RyR₁ sequence with increasing distance from the 3'-end following cDNA synthesis from mRNA. The control reactions to rule

Fig. 3. Comparison of the cDNA nucleotide sequences at the carboxyl-terminus of the RyR₁ for rat (rRyR) and mouse (mRyR). Vertical lines indicate identical nucleotide bases common to the rat and mouse receptor sequences.

rRyR 661 ccaccaggcctgctgacatggatcatgtccatcgatgtcaaataccagatotgaaagtt 720
mRyR 669 ccaccggcctgctgacatggatcatgtctatcgatgtcaaataccagatctgaaagtt 728

rRyR 721 ggagtcatttcacagacaacttttcgttatctggctggatcatggatgttcctc 780
mRyR 729 ggagtcatttcacagacaacttttcgttatctggctggatcatggatgttcctc 788

rRyR 781 ctgggccactacaataacttttcttcgtccaccccttggatatcgccatggagtc 840
mRyR 789 ctggggcactacaataacttttcttcgtccaccccttggatatcgccatggagtc 848

rRyR 841 aagacgcgtgcgaccatccatccgtcactcacaacggaaagcagctggatgaca 900
mRyR 849 aagacggcgtccgaccatccatccgtcactcacaatggaaagcagctggatgaca 908

rRyR 901 gtagggctctggcttagtggttacttgtatcgggtggccctcaactttccgc 960
mRyR 909 gtagggctctggccgttagtggttacttgtatcagtggtggccctcaactttccgc 968

rRyR 961 aagttctacaacaagagcgaagatgaggacgacccgtacatgaagtgtgacatgatg 1020
mRyR 969 aaattctacaacaagagcgaagatgaggacgacccgtacatgaagtgtgacatgatg 1028

rRyR 1021 acgtgtctacctgttccacatgtatgtggcgccggccgggtggcatcggggacgag 1080
mRyR 1029 acgtgtctacctgttccacatgtatgtggcgtccggccgggtggagggatcggggacgag 1088

rRyR 1081 atcgaggaccggcgtgtgtatgaaatataactgttacccgggtcgatccacatcc 1140
mRyR 1089 atcgaggaccggcggcgtatgaaatataactttacccgggtcgatccacatcc 1148

rRyR 1141 ttcttcttcgtcattgtcattctactggctatcatccagggtctgattttatgtgtttc 1200
mRyR 1149 ttcttcttcgttatactgtcattctgtgttgcataccatcagggtctgattttatgtgtttc 1208

rRyR 1201 gggagactccgagaccaacaagagcgaactgtgaaaggacatggagaccaagtgtttc 1260
mRyR 1209 gggagactccgagaccaacaagagcgaactgtgaaaggacatggagaccaagtgtttc 1268

rRyR 1261 tggggataggcagtgactacttcgacacgaccccacatgggtttgagacccacactctg 1320
mRyR 1269 tggggataggcagtgactacttcgacacacccccacatgggtttgagacccacactctg 1328

rRyR 1321 gaagagcacacccatgttttctgtgttattgtatggatggatggatggatggatgg 1380
mRyR 1329 gaagagcacacccatgttttctgtgttattgtatggatggatggatggatggatgg 1388

rRyR 1381 acaggaggcacccggtcaggagtcatacgatggaaatgttacccggaggggtgtggg 1440
mRyR 1389 acaga-gcacactgttcaggagtcgtatgttacccggaggggtgtggg 1447

rRyR 1441 ctctttccctgtggagactgtttccgaaagcagttatgttgcgtggatggatgg 1500
mRyR 1448 ttctttccctgtggagactgtttccgcaagcagttatgttgcgtggatggatggatgg 1507

rRyR 1501 gcagctggccc-tccccccacctaagtcgttccactgtcaagctcccccaggcag 1559
mRyR 1508 gcagctggcccttccccccacctaagtcgttccactgtcaagctcccccaggcag 1566

rRyR 1560 ctggggacagatgtatccgttaacttagaccaa 1589
mRyR 1567 ctggggacagatgtatccgttaacttagaccaa 1596

Fig. 3. Continued.

out genomic DNA contamination performed in the absence of reverse transcriptase did not result in amplification.

The authenticity of each of the amplified bands as RyR₁ fragments was confirmed by sequencing analysis. A total of 1589 bases of the rat RyR₁ were amplified using the 5'-RACE strategy in addition to RT-PCR amplification using primers (+) 5'-gggtgaactggaaagtacagagagtg-3', and (-) 5'-ttggcttagttcaggatcatgtc-3' to mouse brain type RyR sequence. Attempts to extend the sequence further were not

successful. The rat 3-9 cell RyR₁ sequence was 99% homologous with rat brain RyR₁ (GenBank accession no. AF130879) and 95% homologous to mouse RyR₁ (GenBank accession no. X83932) as determined by Blast analysis (Fig. 3). Attempts to identify the rat parotid gland RyR₁ by Western blotting and Northern analysis proved unsuccessful, indicating that the antisera used to identify RyR₁ did not bind to a specific carboxy-terminal epitope on the RyR₁ (see Zhang et al., 1999) and that the expression of the RyR₁ mRNA was below detectable levels.

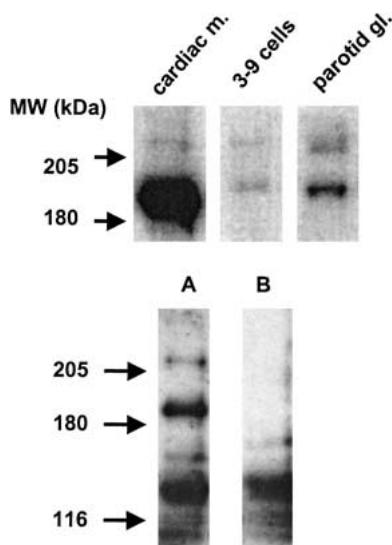


Fig. 4. Expression of VDCC α_1 C subunit proteins in various tissues. In the upper panel, homogenates were analyzed for VDCC α_1 C subunits by electrophoresis through a 5% SDS-polyacrylamide gel and immunoblot in cardiac muscle (*m.*), parotid cell line (3-9 cells), and freshly prepared dispersed rat parotid acinar cells (*gl.*). A high (~210 kDa) and low (~190 kDa) molecular weight form were detected in all tissues. In the lower panel, the specificity of the antibody representing the C-terminal of the anti- α_{1C} subunit was confirmed by immunoblots of rat brain depicting bands corresponding to the high and low molecular weight forms (*A*), which were abrogated after the antibody was mixed with its corresponding peptide (*B*). The position of molecular size markers is indicated by the arrows. The blots shown are representative of three separate experiments.

IDENTIFICATION AND LOCALIZATION OF A DIHYDROPYRIDINE-SENSITIVE CHANNEL

Because RyR is coexpressed with voltage-activated dihydropyridine (DHP)-sensitive Ca^{2+} channels in cardiac and skeletal muscle, and brain (Franzini-Armstrong & Protasi, 1997; Franzini-Armstrong et al., 1999), we tested the hypothesis that a DHP-sensitive Ca^{2+} channel is present in non-muscle cells in association with RyR. Western blot analysis was carried out on homogenates of freshly prepared parotid acinar cells and clonal parotid 3-9 cells using antibody directed against a peptide that represents the C-terminal of the anti- α_{1C} subunit. This subunit functions as the cation channel of the DHPR (Meir et al., 1999). Like cardiac muscle, the antibody recognized a high and a low molecular weight form, with the higher molecular weight form (210 kDa) being present in lesser amounts than the lower molecular weight form (190 kDa) (Fig. 4, upper panel). These values compare favorably with high and low molecular weight forms in skeletal muscle of 214 and 193 kDa, respectively (DeJongh et al., 1991). Moreover, using rat brain as a positive control (Fig. 4*A*, lower panel), we verified the specificity of the antibody by

showing that when it was mixed with its corresponding peptide, bands representing the high and low molecular weight forms were no longer observed (Fig. 4*B*, lower panel). These studies demonstrate that a form of the L-type Ca^{2+} channel is expressed in parotid acinar cells.

To determine the cellular distribution of the DHPR, immunocytochemistry was carried out using frozen sections of parotid glands. Intact acini rather than cultured cells were employed in these experiments in order to localize the fluorescent signal to a specific cytoplasmic component of the acinar cell. Confocal microscopy revealed that acini exposed to anti- α_{1C} subunit antibody displayed a fluorescence that was most prominent in the apical portion of the cell (Fig. 5*A*). A diffuse signal of rather homogeneous intensity was also observed throughout the basal region of the cell; however, the intensity of the fluorescence was clearly weaker than in the apical region. No signal was detected when the primary antibody was preincubated with the antigenic peptide or in the absence of primary antibody (*data not shown*). By comparison, IP₃R_s identified by antiserum specific to subtype II, which is the most abundant subtype (circa 90%) (Zhang et al., 1999), were primarily distributed in the apical pole of the parotid cell (Fig. 5*B*). As previously reported (Zhang et al., 1999), the use of fluorescently labeled BODIPY-ryanodine showed that the highest levels of RyR expression were localized to the basal pole of the cell, and RyR expression was completely absent in the most apical aspect of the cell (Fig. 5*C*). Thus, in parotid cells the DHPR primarily co-localizes with the IP₃R, rather than with the RyR. The localization of the RyR observed in our studies for parotid cells coincides with that reported for exocrine cells of the pancreas in that the RyR was predominantly localized to the basal aspect of the exocrine cell and excluded from the extreme apex of the cell called the trigger zone (Leite et al., 1999; Straub, Giovannucci & Yule, 2000). The trigger zone is the region of the exocrine cell where agonist-induced Ca^{2+} signals are initiated (Tojyo, Tanimura & Matsumoto, 1997; Straub et al., 2000).

Discussion

Because Ca^{2+} regulates a number of diverse cellular processes, the properties of the Ca^{2+} signal encompass a varied number of Ca^{2+} release events, including those involving the RyR. Our previous work utilizing the exocrine cells of the rat parotid gland tentatively identified a RyR₁ isoform by RT-PCR and described its intracellular distribution by cytochemical analysis (Zhang et al., 1997, 1999). The present study broadens this analysis by using RT-PCR to demonstrate the expression of an RyR₁-like mRNA in a number of other non-muscle cells, in-

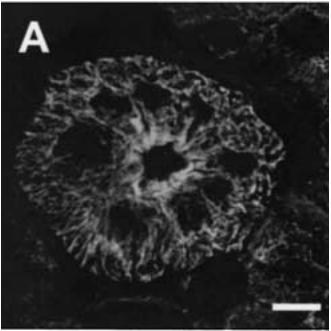
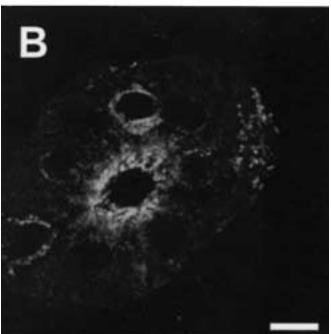
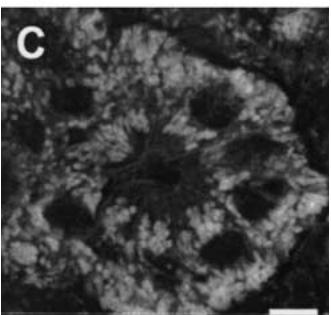
DHPR**IP3R****RyR**

Fig. 5. Confocal images demonstrating the fluorescence localization of DHPR, IP₃R, and RyR in rat parotid gland. Representative images of acini treated with: (A) Ca²⁺ channel antibody (anti- $\alpha 1C$); (B) 1:20 dilution of affinity-purified polyclonal inositol trisphosphate receptor subtype II (IP₃R) rabbit clonal antisera; and (C) 25 μ M BODIPY-ryanodine (reproduced with permission from Zhang et al., 1999, Biochem. J. 340, p. 521, Fig. 1A. © The Biochemical Society). Scale bar 10 μ m. Similar results were obtained in three other experiments.

cluding pancreatic exocrine and endocrine cells, and liver. In another study, an RyR₁ was identified in non-excitable lymphocytes by immunoblotting and molecular biological techniques (Sei, Gallagher & Basile, 1999).

In addition to demonstrating that a brain/skeletal muscle-type RyR₁ mRNA is present in several rat tissues and cell lines, the present study utilized 5'-RACE analysis of parotid cells to extend the sequence of the RyR₁ to 1589 bases. High homology

exists between the rat parotid cell sequence and mouse skeletal muscle RyR₁. Unfortunately, perhaps because of secondary structures, GC-rich sequences, or even an absence of sequence, the 5'-RACE analysis was unable to extend the sequence any further than reported.

In order to obtain evidence for a full-length RyR₁ in non-muscle tissues, primers were designed from a sequence recently reported for the 5'-end of rat skeletal muscle RyR₁ (Martin et al., 1999). As expected, the primer sequence in proximity to the 5'-end of RyR₁ amplified skeletal muscle and brain mRNAs. Surprisingly, several tissues that expressed mRNA with high sequence homology to 3'-end rat brain RyR₁ failed to express a sequence near the 5'-end of RyR₁. These data suggest that the 5'-end of RyR₁ in tissues such as parotid cells, pancreatic islet β -cells, and liver was either not present or differed in sequence such that those primers were not recognized. Precedent for the expression of a truncated form of RyR₁ exists in the novel brain-type RyR₁ which contains only ~2000 base pairs as compared to skeletal muscle RyR mRNA which is composed of ~16,000 nucleotides (Takeshima et al., 1993). Although the functional role of this variant has not been characterized, the brain protein contains the C-terminal region which is thought to express the Ca²⁺ channel domain but lacks the "foot" region (Takeshima et al., 1993; Furuichi et al., 1994).

Previous studies from our laboratory suggested that the RyR identified in parotid exocrine cells differs in its functional properties from those of authentic RyR₁ (Zhang et al., 1997, 1999). Unlike classical RyR₁, the parotid cell RyR lacked a sensitivity to caffeine, and ryanodine failed to open the RyR/channel at low concentrations or block the channel in higher concentrations in permeabilized parotid cells (Zhang et al., 1997). Morphologically, the expression of an RyR high-affinity binding site was demonstrated in parotid acini by confocal microscopy using the fluorophore BODIPY-ryanodine and by [³H]ryanodine binding (Zhang et al., 1997, 1999). However, the finding that cADPR and cAMP markedly reduced [³H]ryanodine binding (Zhang et al., 1999) contrasts with studies showing that adenine nucleotides, including cADPR, either enhance, inhibit, or have negligible effects on [³H]ryanodine binding in muscle and nerve (Fruen et al., 1994; Zucchi & Ronca-Testoni, 1997; Shoshan-Barmatz & Ashley, 1998; Hadad et al., 1999). Such evidence portrays a RyR₁ isoform in parotid cells that possesses less complex regulatory mechanisms compared to full-length RyR₁ (see Furuichi et al., 1994). The notion favoring the existence of a novel RyR isoform was supported by Western blot analysis of parotid cell membranes using antibodies raised against type -I, -II, and -III RyRs, which failed to demonstrate protein bands that have electrophoretic

mobility patterns similar to that of the RyR (Zhang et al., 1999). It is noteworthy that comparative studies of the channel properties of mammalian RyR isoforms and isoforms expressed in chicken, frog, fish, and lobster muscle have revealed diversity in the gating and activation of the channels (Sutko et al., 1997). This diversity underlies different roles in Ca^{2+} signaling for each RyR isoform, including the parotid RyR₁.

Besides IP₃- and ryanodine-induced Ca^{2+} release, L-type Ca^{2+} channels may also play a functional role in parotid cells. The present study reveals that a form of the α_1 polypeptide associated with voltage-gated Ca^{2+} channels of excitable cells is also expressed in parotid acinar cells. Western blot analysis identified two forms of the peptide, with the lower molecular weight form present in higher levels (*see* Fig. 4). The fact that these two forms of the α_1 subunit of DHPR are of a size comparable to those identified in muscle and nerve (Catterall, 1997) suggests that L-type channels in parotid cells share certain structural and/or functional properties with those in excitable cells. Although pharmacological evidence does not support the presence of a muscle- or nerve-type of voltage-dependent Ca^{2+} channel in exocrine acinar cells (Putney, 1981; Williams & Burnham, 1985), the report that murine erythroleukemia cells express a truncated form of the α_1 subunit of the cardiac voltage-gated Ca^{2+} channel (Ma, Kobrinsky & Marks, 1995) is consistent with the concept that non-excitable cells express a DHPR that is somehow linked to mechanisms regulating Ca^{2+} signaling.

Although the mechanism of coupling between L-type Ca^{2+} channels and RyRs differs in skeletal and cardiac muscle (*see* Introduction), there is tight coupling between L-type channels and RyRs in both tissues. By contrast, in smooth muscle cells L-type channels are loosely coupled to RyRs by virtue of an increase in the effective distance between the Ca^{2+} channel and RyR (Collier, Wang & Kotlikoff, 2000). These findings lead to the conclusion that the interaction between RyR and DHPR is tissue-specific (*see* also Bhat et al., 1997b). The mechanism of Ca^{2+} gating in the parotid acinar cell may primarily involve coupling of the L-type channels to IP₃Rs in the apical pole where both proteins predominate. The fact that the RyR and DHPR are not colocalized to a large extent in the parotid cell is in accord with our other major finding that the parotid cell (as well as certain other cells/tissues) possess a variant of the RyR₁ that may be devoid of at least a portion of the foot region (5'-region). The foot region is a component of the RyR/channel responsible for linking the RyR to the DHPR (Franzini-Armstrong & Protasi, 1997; Franzini-Armstrong et al., 1999). On the other hand, our results do not preclude the possibility that the relatively weak fluorescent signal in the basal region of the cell may reflect colocalization of the DHPR

with the RyR. In this case, the immunoreactivity observed in both the apical and to a lesser extent in the basal portion of the cell may represent the low and high molecular weight forms, respectively, of the α_{1C} subunit, which are differentially localized in the parotid acinar cell and perform diverse functions. Several lines of evidence favor the concept that DHPRs can regulate the activity of IP₃Rs (Mackrill, 1999). On the basis of the structural similarity in the C-terminal (channel) region of the IP₃Rs and RyRs (Takeshima, 1993), as well as functional studies, Spat, Rohacs & Hunyady (1994) postulated that IP₃Rs interact with DHPRs in the endoplasmic reticulum of rat adrenal glomerulosa cells in a manner analogous to that occurring between the RyR and DHPR in skeletal muscle. Spat et al. (1996) also theorized that, since the L-type channel serves as a voltage sensor in skeletal muscle, in a non-excitable cell (one not activated by depolarization), IP₃R function must be regulated by a variant of the L-type channel. In this connection, Zhang and O'Neil (1996) demonstrated a Ca^{2+} channel in the apical membrane of rabbit renal epithelial cells that is DHP-sensitive and activated by membrane depolarization. However, compared with a typical L-type channel in excitable cells, the renal channel manifested certain diverse properties, including a relatively small channel size (Zhang & O'Neil, 1996). Thus a variant of the typical L-type channel may also operate in parotid cells to modulate IP₃-induced Ca^{2+} mobilization or store-operated Ca^{2+} entry, where Ca^{2+} influx is regulated by the filling of depleted intracellular Ca^{2+} stores (Parekh & Penner, 1997). Functional studies are planned to address these possible interactions.

The parotid acinar cell is polarized such that the endoplasmic reticulum and nucleus are located in the basal region of the cell, whereas the apical region harbors the zymogen granules. It is interesting that carbachol stimulation of parotid acinar cells results in the initiation of a Ca^{2+} wave at the apical pole, which spreads toward the basal pole despite the fact that agonists that induce IP₃ production exert their primary action on the basal aspect of the acinar cell surface (Tojyo, Tanimura & Matsumoto, 1997; Liu, Scott & Smith, 1998). In attempting to explain these findings, one may speculate that the DHPR that we have identified in the parotid cell may be a contributory factor to the greater sensitivity to Ca^{2+} release exhibited by IP₃ in the apical region (Tanimura, Matsumoto & Tojyo, 1998).

In conclusion, the present and previous studies have identified what is perhaps a variant of RyR₁, along with three IP₃R isoforms and two DHPR subtypes in parotid acinar cells (Zhang et al., 1997, 1999). The identification of these key elements represents a potentially important step in gaining a deeper understanding of the mechanisms regulating Ca^{2+} signaling in non-excitable cells.

These studies were supported in part by the NIH research grant DE-059654 to RPR and a grant from the American Diabetes Association to SGL. BL was supported by a fellowship from The Juvenile Diabetes Foundation International. We thank Dr. Keshore Bidasee of Indiana University School of Medicine for carrying out multiple sequence analysis of RT-PCR product and Dr. Xuejun Zhang for designing several primers. We also thank Dr. Richard Wojcikiewicz of Upstate Medical University at Syracuse (New York) for generously supplying the IP₃R antiserum specific to subtype II.

References

- Bennett, D.L., Cheek, T.R., Berridge, M., DeSmedt, H., Parys, J.B., Missiaen, L., Bootman, M.D. 1996. Expression and function of ryanodine receptors in nonexcitable cells. *J. Biol. Chem.* **271**:6356–6362
- Bhat, M.B., Zhao, J.Y., Takeshima, H., Ma, J. 1997a. Functional calcium release channel formed by the carboxyl-terminal portion of ryanodine receptor. *Biophys. J.* **73**:1329–1336
- Bhat, M.B., Zhao, J., Zang, W., Balke, C.W., Takeshima, H., Wier, W.G., Ma, J. 1997b. Caffeine-induced release of intracellular calcium from Chinese hamster ovary cells expressing skeletal muscle ryanodine receptor. Effects on full-length and carboxy-terminal portion of calcium release channels. *J. Gen. Physiol.* **110**:749–762
- Catterall, W.A. 1997. Modulation of sodium and calcium channels by protein phosphorylation and G proteins. In: Signal Transduction in Health and Disease. Adv. Second Messenger and Phosphoprotein Research Vol. 31. J. Corbin, S. Francis, editors. pp. 159–181, Lippincott-Raven Publishers, Philadelphia
- Collier, M.L., Wang, Y.X., Kotlikoff, M.I. 2000. Calcium-induced calcium release in smooth muscle: Loose coupling between the action potential and calcium release. *J. Gen. Physiol.* **115**:653–662
- DeJongh, K.S., Warner, C., Colvin, A.A., Catterall, W.A. 1991. Characterization of the two size forms of the $\alpha 1$ subunit of skeletal muscle L-type calcium channels. *Proc. Natl. Acad. Sci. USA* **88**:10778–10782
- DiJulio, D.H., Watson, E.L., Pessah, I.N., Jacobson, K.L., Ott, S.M., Buck, E.D., Singh, J.C. 1997. Ryanodine receptor type III (RyR₃) identification in mouse parotid acini. *J. Biol. Chem.* **272**:15687–15696
- Franzini-Armstrong, C., Protasi, F. 1997. Ryanodine receptors of striated muscles: a complex channel capable of multiple interactions. *Physiol. Rev.* **77**:699–729
- Franzini-Armstrong, C., Protasi, F., Ramesh, V. 1999. Shape, size, and distribution of Ca²⁺ release units and couplons in skeletal and cardiac muscles. *Biophys. J.* **77**:1528–1549
- Fruen, B.R., Mickelson, J.R., Shomer, N.H., Velez, P., Louis, C.F. 1994. Cyclic ADP-ribose does not affect cardiac or skeletal muscle ryanodine receptors. *FEBS Lett.* **352**:123–126
- Furuichi, T., Kohda, K., Miyawaki, A., Mikoshiba, K. 1994. Intracellular channels. *Curr. Opin. Neurobiol.* **4**:294–303
- Giannini, G., Clementi, E., Ceci, R., Marziali, G., Sorrentino, V. 1992. Expression of a ryanodine receptor-Ca²⁺ channel that is regulated by TGF- β . *Science* **257**:91–94
- Giannini, G., Conti, A., Mammarella, S., Scrobogna, M., Sorrentino, V. 1995. The ryanodine/calcium channel genes are widely and differentially expressed in murine brain and peripheral tissues. *J. Cell Biol.* **128**:893–904
- Hadad, N., Martin, C., Ashley, R.H., Shoshan-Barmatz, S. 1999. Characterization of sheep brain ryanodine receptor ATP binding site by photoaffinity labeling. *FEBS Lett.* **455**:251–256
- Hell, J.W., Westenbroek, R.E., Warner, C., Ahlijanian, M.K., Prystay, W., Gilbert, M.M., Snutch, T.P., Catterall, W.A. 1993. Identification and differential subcellular localization of the neuronal class C and class D L-type calcium channel $\alpha 1$ subunits. *J. Cell Biol.* **123**:949–962
- Holz, G.G., Leech, C.A., Heller, R.S., Castonguay, M., Habener, J.F. 1999. cAMP-dependent mobilization of intracellular Ca²⁺ stores by activation of ryanodine receptors in pancreatic β -cells. *J. Biol. Chem.* **274**:14147–14156
- Leite, M.F., Dranoff, J.A., Gao, L., Nathanson, M.H. 1999. Expression and subcellular localization of the ryanodine receptor in rat pancreatic acinar cells. *Biochem. J.* **337**:305–309
- Liu, P., Scott, J., Smith, P.M. 1998. Intracellular calcium signaling in rat parotid acinar cells that lack secretory vesicles. *Biochem. J.* **330**:847–852
- Ma, Y., Kobrinsky, F., Marks, A.R. 1995. Cloning and expression of a novel truncated calcium channel from non-excitable cells. *J. Biol. Chem.* **270**:483–493
- Mackrill, J.J. 1999. Protein-protein interactions in intracellular Ca²⁺-release channel function. *Biochem. J.* **337**:345–361
- Martin, C., Hyvelin, J.-M., Chapman, K.E., Marthan, R., Ashley, R.H., Savineau, J.P. 1999. Pregnant rat myometrial cells show heterogeneous ryanodine- and caffeine-sensitive calcium stores. *Amer. J. Physiol.* **227**:C243–C252
- Meir, A., Ginsburg, S., Butkevich, A., Kachalsky, S.G., Kaiserman, I., Ahdut, R., Demirgoren, S., Rahamimoff, R. 1999. Ion channels in presynaptic nerve terminals and control of transmitter release. *Physiol. Rev.* **79**:1019–1088
- Parekh, A., Penner, R. 1997. Store depletion and calcium influx. *Physiol. Rev.* **77**:901–930
- Putney J.W. Jr. 1981. Calcium antagonists and calcium-gating mechanisms in the exocrine glands. In: New Perspectives on Calcium Antagonists; G.B. Weiss editor. pp. 169–175. American Physiological Society, Bethesda, Maryland.
- Rubin, R.P., Adolf, M.A. 1994. Cyclic AMP regulation of calcium mobilization and amylase release from isolated permeabilized rat parotid cells. *J. Pharmacol. Exp. Ther.* **268**:600–606
- Sei, Y., Gallagher, K.L., Basile, A.S. 1999. Skeletal muscle type ryanodine receptor is involved in calcium signaling in human B lymphocytes. *J. Biol. Chem.* **274**:5995–6002
- Shoshan-Barmatz, V., Ashley, R.H. 1998. The structure, function, and cellular regulation of ryanodine-sensitive Ca²⁺ release channels. *Int. Rev. Cytology* **183**:185–270
- Spat, A., Rohacs, T., Hunyady, L. 1994. Plasmalemmal dihydropyridine receptors modify the function of subplasmalemmal inositol 1,4,5-trisphosphate receptors: a hypothesis. *Cell Calcium* **15**:431–437
- Spat, A., Rohacs, T., Horvath, A., Szabadkai, G.Y., Enyedi, P. 1996. The role of voltage-dependent calcium channels in angiotensin-stimulated glomerulosa cells. *Endocrine Res.* **22**:569–576
- Straub, S.V., Giovannucci, D.R., Yule, D.I. 2000. Calcium wave propagation in pancreatic acinar cells. Functional interaction of inositol 1,4,5-trisphosphate receptors, ryanodine receptors, and mitochondria. *J. Gen. Physiol.* **116**:547–559
- Sundaresan, S., Weiss, J., Bauer-Dantoin, A.C., Jameson, J.L. 1997. Expression of ryanodine receptors in the pituitary gland: Evidence for a role in gonadotropin-releasing hormone signaling. *Endocrinology* **138**:2056–2065
- Sutko, J.L., Airey, J.A. 1996. Ryanodine receptor Ca²⁺ release channels: does diversity in form equal diversity in function? *Physiol. Rev.* **76**:1027–1071
- Sutko, J.L., Airey, J.A., Welch, W., Ruest, L. 1997. The pharmacology of ryanodine and related compounds. *Pharmacol. Rev.* **49**:53–98

- Takeshima, H. 1993. Primary structure and expression from cDNAs of the ryanodine receptor. *Ann. N.Y. Acad. Sci.* **707**:165–177
- Takeshima, H., Nishimura, S., Nishi, M., Ikeda, M., Sugimoto, T. 1993. A brain-specific transcript from the 3'-terminal region of the skeletal muscle ryanodine receptor gene. *FEBS Lett.* **322**:105–110
- Tanimura, A., Matsumoto, Y., Tojyo, Y. 1998. Polarized Ca^{2+} release in saponin-permeabilized parotid acinar cells evoked by flash photolysis of ‘caged’ inositol 1,4,5-trisphosphate. *Biochem. J.* **332**:769–772
- Tojyo, Y., Tanimura, A., Matsumoto, Y. 1997. Imaging of intracellular Ca^{2+} waves induced by muscarinic receptor stimulation in rat parotid acinar cells. *Cell Calcium* **22**:455–462
- Tunwell, R.E.A., Lai, F.A. 1996. Ryanodine receptor expression in the kidney and a non-excitable kidney epithelial cell. *J. Biol. Chem.* **271**:29583–29588
- Williams, J.A., Burnham, D.B. 1985. Calcium and stimulus-secretion coupling in pancreatic acinar cells. In: *Calcium in Biological Systems*. R.P. Rubin, G.B. Weiss, J.W., Jr. Putney, editors. pp. 83–91. Plenum Press, New York
- Zhang, M.I.N., O’Neil, R.G. 1996. An L-type calcium channel in renal epithelial cells. *J. Membrane Biol.* **154**:259–266
- Zhang, X., Wen, J., Bidasee, K.R., Besch, H.R. Jr., Rubin, R.P. 1997. Ryanodine receptor expression is associated with intracellular Ca^{2+} release in rat parotid acinar cells. *Amer. J. Physiol.* **273**:C1306–C1314
- Zhang, X., Wen, J., Bidasee, K.R., Besch, H.R. Jr., Wojcikiewicz, R.J.H., Lee, B., Rubin, R.P. 1999. Ryanodine and inositol trisphosphate receptors are differentially distributed and expressed in rat parotid gland. *Biochem. J.* **340**:519–527
- Zhu, Y., Aletta, J.M., Wen, J., Zhang, X., Higgins, D., Rubin, R.P. 1998. Rat serum induces a differentiated phenotype in a rat parotid acinar cell line. *Amer. J. Physiol.* **275**:G259–G268
- Zucchi, R., Ronca-Testoni, S. 1997. The sarcoplasmic reticulum Ca^{2+} channel/ryanodine receptor: modulation by endogenous effectors, drugs, and disease states. *Pharmacol. Rev.* **49**:1–51